

One-dimensional acoustic waves in air/water mixtures

C.L.Farmer, H.Ockendon, J.R.Ockendon

Mathematical Institute, University of Oxford, Oxford, OX2 6GG

Abstract

Homogenisation theory is used to derive Wood's formula for the speed at which a pressure wave can propagate in an air/water mixture. The smallness of the impedance ratio between air and water results in a dramatic lowering of the wave speed of the mixture and, when the air fraction is small, the possibility of regions of persistent ringing in the vicinity of the boundary where the pressure is applied. Only Goupillaud media are considered and, for the periodic case, the asymptotic predictions are validated against exact numerical calculations. An example in which the air/water layers vary randomly is also presented.

Keywords: waves, layered medium

1. Introduction

There is a long-standing literature concerning propagation of sound waves through air/water mixtures, much of which is concerned with the dependence of attenuation and dispersion on the frequency of insonification. In this paper we will consider the one-dimensional propagation of a sound wave along a tube containing a periodic distribution of slugs of air and water. In this situation it is known that the effect of even a small fraction of one medium in the other can change the value of the sound speed dramatically. Our primary objective is to understand this phenomenon as simply as possible in the time domain using the mathematical theory of homogenisation. We also describe the effect of the small density ratio on the response of a semi-infinite mixture to a constant applied pressure, and, for a specific class of problems, we compare these results with exact numerical computations.

We will consider air/water regions spaced periodically in a tube $0 < X < \infty$. The acoustic equations for a perfect gas with reference density and pressure ρ_{a0} and p_{a0} , are

$$\frac{\partial p_a}{\partial T} + \frac{\partial u_a}{\partial X} = 0 \quad (1)$$

and

$$\frac{\partial u_a}{\partial T} + \frac{\partial p_a}{\partial X} = 0, \quad (2)$$

15 where $p_{a0}(1 + \epsilon p_a)$ and $\rho_{a0}(1 + \epsilon \rho_a)$ are the pressure and density, ϵp_{a0} is determined by the imposed excess pressure at $X = 0$, $\epsilon \sqrt{\frac{p_{a0}}{\gamma_a \rho_{a0}}} u_a$ is the velocity and $p_a = \gamma_a \rho_a$, where $\gamma_a \simeq 1.4$ is the ratio of specific heats. The length has been scaled with the period of the medium and the time scale has been chosen so that the non-dimensional speed of sound in air is unity.

In water, the gas law must be replaced by an equation of state that models its near incompressibility. We select for definiteness the Murnaghan equation of state [1]

$$\frac{p}{p_{w0}} = 1 + \lambda \left(\left(\frac{\rho}{\rho_{w0}} \right)^{\gamma_w} - 1 \right), \quad (3)$$

where p_{w0} and ρ_{w0} are the reference values of pressure and density, $\lambda \simeq 3 \times 10^3$ and $\gamma_w \simeq 7$. Writing the water pressure and density as $p_{w0}(1 + \epsilon p_w)$ and $\rho_{w0}(1 + \epsilon \rho_w)$, the velocity as $\epsilon \sqrt{\frac{p_{a0}}{\gamma_a \rho_{a0}}} u_w$, and taking $p_{w0} = p_{a0}$, the acoustic equations in the water are

$$\delta \frac{\partial p_w}{\partial T} + c^2 \frac{\partial u_w}{\partial X} = 0 \quad (4)$$

and

$$\frac{\partial u_w}{\partial T} + \delta \frac{\partial p_w}{\partial X} = 0, \quad (5)$$

where $c = \sqrt{\frac{\lambda \gamma_w \rho_{a0}}{\gamma_a \rho_{w0}}}$ is the speed of sound in water relative to that in air and is experimentally observed to be approximately 3.5. The density ratio at an interface is $\delta = \frac{\rho_{a0}}{\rho_{w0}} \simeq 10^{-3}$ and the impedance ratio of air to water is

$$\frac{\rho_{a0} c_{a0}}{\rho_{w0} c_{w0}} = \sqrt{\frac{\gamma_a \rho_{a0}}{\lambda \gamma_w \rho_{w0}}} = O(10^{-4}). \quad (6)$$

20 As is usual in acoustic analysis, the mass and momentum conservation equations uncouple from the energy equation.

The boundary conditions at an air/water interface that ensure continuity of mass and momentum are

$$p_w = p_a, \quad u_w = u_a, \quad (7)$$

and, in general, there will be jump discontinuities in the first derivatives of these variables at the interfaces.

In this paper we consider the simple configuration in which a constant non-zero
 25 pressure is applied at $X = 0$ for $T > 0$ to an air/water mixture which is initially at
 rest at pressure p_{a0} .¹ Although the effect of the pressure disturbance will involve a
 leading wave that travels at the sound speeds in air and water alternately, the theory of
 homogenisation in periodic layered media reveals that, because of wave reflection at
 the interfaces, the most significant disturbance lags behind the leading disturbance and
 30 travels at a ‘homogenised’ wave speed c_H . As shown in, for example, [7], for a layered
 medium in which $\delta = 1$, the inverse of the square of the homogenised wave speed is the
 mean of the inverse squares of the two original wave speeds. The papers [5], [6] give
 a comprehensive description of the theory and its numerical implementation for other
 values of δ . Our aim is to study, both analytically and numerically, how a small density
 35 ratio δ can not only result in the homogenised wavespeed being much slower than the
 speed of sound in either medium, but can also affect the regions in space and time in
 which homogenisation is valid.

2. Formal Homogenisation Analysis

Throughout this paper we will assume that δ is small, but, in order to consider long
 40 timescales over which to homogenise, we need to introduce a second small parameter
 τ^{-1} , against which δ will need to be compared. We will find that our predictions depend
 crucially on the air fraction α and, to begin with, we will assume that neither α nor $(1-\alpha)$
 is small, although this assumption will be relaxed in Section 3.3.

We suppose that air is contained in the regions $n < X < n + \alpha$ and water is in

¹We will see that the discontinuity in this boundary condition at $t = 0$ means that (7) will not hold at all times on the interfaces.

regions $n + \alpha < X < n + 1$ where n is an integer ≥ 0 . We note that (1, 2, 4, 5) can be combined into the single scalar equation

$$K \frac{\partial}{\partial X} \left(\frac{1}{\rho} \frac{\partial \phi}{\partial X} \right) = \frac{\partial^2 \phi}{\partial T^2}, \quad (8)$$

where ϕ is either of the dependent variables. For elastic waves, K would be the bulk modulus and ρ is the density. When ϕ is the pressure in our problem, then, in the air,

$$\phi = p_a, \rho = K = 1 \quad \text{for} \quad n < X < n + \alpha \quad (9)$$

and in the water,

$$\phi = p_w, \rho = \frac{1}{\delta}, K = \frac{c^2}{\delta} \quad \text{for} \quad n + \alpha < X < n + 1. \quad (10)$$

Alternatively, if ϕ is the velocity, then K and ρ take different values although $\frac{K}{\rho}$ is still
45 the square of the speed of sound in each region. The numerical and analytical solutions of (8) when $\delta = 1$ have been considered in [7] and the solutions of two-dimensional versions of (8) have been described by [5], [6], [8].

We will mostly consider the boundary and initial conditions used in [7] namely

$$\phi = 1 \quad \text{at} \quad X = 0 \quad \text{for} \quad T > 0 \quad \text{and} \quad \phi = \frac{\partial \phi}{\partial T} = 0 \quad \text{at} \quad T = 0 \quad \text{for} \quad X > 0. \quad (11)$$

This means that the boundary pressure is applied to an air layer, and, except at the end of Section 3.3, this is the configuration we will consider throughout this paper.

We write the formal asymptotic expansion

$$\phi \sim \sum_{k=0}^{\infty} \tau^{-k} \phi_k(x, X, t), \quad (12)$$

where $x = \frac{X}{\tau}$ and $t = \frac{T}{\tau}$ and τ is the timescale of the observer, which is long compared to the time for a wave to traverse a single period of the medium, i.e. $\tau \gg 1$. As in [7], we would need ϕ_k to also depend on T if the boundary data varied on the T -scale. We carry out the homogenisation on the first-order system (1,2,4,5) written as

$$\frac{\partial p}{\partial T} + K \frac{\partial u}{\partial X} = 0 \quad (13)$$

and

$$\rho \frac{\partial u}{\partial T} + \frac{\partial p}{\partial X} = 0, \quad (14)$$

50 where K and ρ are defined as in (9),(10).

Replacing $\frac{\partial}{\partial X}$ by $\frac{\partial}{\partial X} + \frac{1}{\tau} \frac{\partial}{\partial x}$ and $\frac{\partial}{\partial T}$ by $\frac{1}{\tau} \frac{\partial}{\partial t}$, and expanding u and p as in (12) gives, to the lowest order,

$$\frac{\partial u_0}{\partial X} = \frac{\partial p_0}{\partial X} = 0, \quad (15)$$

so that $u_0 = u_0(x, t)$ and $p_0 = p_0(x, t)$. This means that u_1 and p_1 satisfy

$$\frac{\partial u_1}{\partial X} = -\frac{\partial u_0}{\partial x} - \frac{1}{K} \frac{\partial p_0}{\partial t} \quad (16)$$

and

$$\frac{\partial p_1}{\partial X} = -\frac{\partial p_0}{\partial x} - \rho \frac{\partial u_0}{\partial t}. \quad (17)$$

Hence, if u_1 and p_1 are not to grow indefinitely as $X \rightarrow \infty$, the average over a period in X of the right-hand sides of (16) and (17) must be zero. Thus u_0 and p_0 must both satisfy the wave equation

$$\frac{\partial^2 \phi_0}{\partial x^2} = \frac{1}{c_H^2} \frac{\partial^2 \phi_0}{\partial t^2}, \quad (18)$$

with

$$\frac{1}{c_H^2} = \frac{\rho_{AV}}{K_H}, \quad (19)$$

where

$$\frac{1}{K_H} = \overline{\left(\frac{1}{K}\right)} \quad \text{and} \quad \rho_{AV} = \overline{(\rho)}, \quad (20)$$

and the overbar denotes the average over a unit cell of air and water. The boundary and initial conditions when $\phi_0 = p_0$ are

$$\phi_0 = 1 \quad \text{on} \quad x = 0, t > 0, \quad \phi_0 = \frac{\partial \phi_0}{\partial t} = 0 \quad \text{on} \quad t = 0, x > 0. \quad (21)$$

The averages can be calculated directly and we find that

$$\frac{1}{c_H^2} = \frac{1}{\delta} (1 - \alpha + \delta \alpha) \left(\alpha + \frac{(1 - \alpha)\delta}{c^2} \right). \quad (22)$$

This formula is well-known in the theory of bubbly liquids as Wood's Law². It gives a good fit with, for example, the experimental observations cited by [9]. When δ is

²Although this is the commonly used name [2], the same expression was derived earlier by Mallock [3].

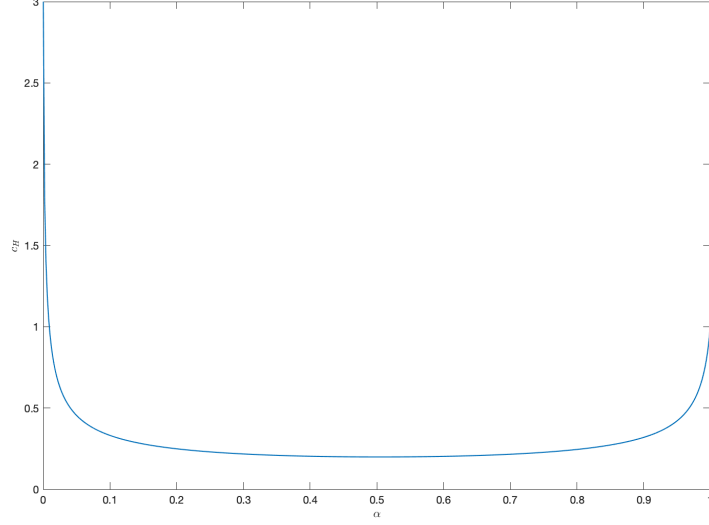


Figure 1: c_H as a function of α when $\delta = 10^{-2}$ and $c = 3$.

small, (22) reveals the surprising result, illustrated in Figure 1, that unless α or $(1 - \alpha)$ is of $O(\delta)$, the value of c_H is $O(\sqrt{\delta})$ and is thus an order of magnitude smaller than the
55 sound speeds in either air or water³.

It was shown in [7] that, in an example where $\delta = 1$, (18) does not hold uniformly as $t \rightarrow \infty$. In a region near $x = c_H t$ in which $x - c_H t$ is of $O(1)$ but $t = O(\tau^2)$, the homogenised step-function wave disperses into a smooth waveform which is the solution of the equation

$$A \frac{\partial^4 \phi_0}{\partial \zeta^4} = \frac{\partial^2 \phi_0}{\partial \hat{t} \partial \zeta}, \quad (23)$$

where $\zeta = x - c_H t$, $t = \tau^2 \hat{t}$ and A is a constant. For any δ of $O(1)$ the resulting waveform is thus the integral of an Airy function whose argument is proportional to $\frac{\zeta}{\hat{t}^{2/3}}$. A similar calculation to that carried out in [7] to determine how A depends on α and c as $\delta \rightarrow 0$ is outlined in the Appendix. However, the fact that $c_H \rightarrow 0$ as $\delta \rightarrow 0$ poses the question of

³An audible demonstration is described in [4].

60 what happens when the most significant part of the homogenised wave moves relatively slowly and we will consider this case in Sections 3.1 and 3.2 when neither α nor $(1 - \alpha)$ is small. Then, in Section 3.3, we will consider the modification necessary when α or $(1 - \alpha)$ is of $O(\delta)$. Finally in Section 4 we will compare these asymptotic predictions with exact numerical calculations.

65 3. A Model for a Goupillaud Medium

For our configuration in which a constant pressure $p = 1$ is applied at $X = 0$ for $T \geq 0$, (1, 2, 4, 5) have piecewise constant solutions. In order to make analytical and computational progress we only consider a ‘Goupillaud’ medium, which is characterised by the fact that $\frac{c\alpha}{(1 - \alpha)}$ is rational. As shown in Section 4, this guarantees the periodicity of the characteristic pattern in the (X, T) plane and the existence of regions periodic in X across which the travel time for a wave is always the same. A simple geometric pattern emerges when $\alpha = (1 + c)^{-1}$, in which case the periodicity is 1 in the X -direction, 2α in the T -direction and the average characteristic speed in a period is

$$c_{AV} = \frac{c}{c\alpha + 1 - \alpha} = \frac{1}{2}(1 + c). \quad (24)$$

In this special case the characteristic pattern is as shown in Figure 2, where $X = m$ and $T = n/c_{AV}$ at the lowest vertex of each shaded region. The pressure and velocity in each of these regions are constant and are denoted by $p_{m,n}$ and $u_{m,n}$ and knowledge of these variables allows the values in the remaining cells to be inferred directly. Had the
70 pressure been applied to a water layer the characteristic pattern would be as in Figure 2 for $X > \alpha$.

3.1. The Exact Solution

We can solve (1, 2, 4, 5) exactly in the air and water and then use the continuity of p and u at the interfaces to derive the difference equations

$$(c + \delta)(p_{m,n+1} - u_{m,n+1}) = (c - \delta)(p_{m,n} + u_{m,n}) + 2(\delta p_{m+1,n} - c u_{m+1,n}) \quad (25)$$

for $m, n \geq 0$, and

$$(c + \delta)(p_{m,n+1} + \frac{c}{\delta} u_{m,n+1}) = 2c(p_{m-1,n} + u_{m-1,n}) - (c - \delta)(p_{m,n} - \frac{c}{\delta} u_{m,n}) \quad (26)$$

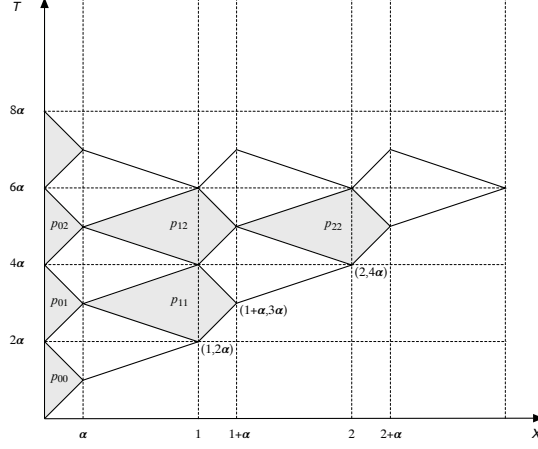


Figure 2: Characteristics in a Goupillaud medium when $\alpha = \frac{1}{1+c}$ and $c_{AV} = \frac{1+c}{2} = \frac{1}{2\alpha}$.

for $m \geq 1, n \geq 0$. We also know that

$$p_{m,n} = u_{m,n} = 0 \quad \text{if } m > n, \quad (27)$$

and

$$p_{0,n} = 1 \quad \text{for } n \geq 0. \quad (28)$$

Hence $u_{m,n}$ and $p_{m,n}$ can be calculated for all $m, n \geq 0$.

A solution of these difference equations is

$$p_{m,n} = P \lambda^m \mu^n, \quad u_{m,n} = U \lambda^m \mu^n, \quad (29)$$

where P, U and λ are all functions of μ , and $\lambda(\mu)$ satisfies

$$\lambda^2 - 2\lambda S(\mu) + 1 = 0 \quad (30)$$

with

$$2S(\mu) = \frac{(c+\delta)^2 \mu}{4c\delta} - \frac{(c-\delta)^2}{2c\delta} + \frac{(c+\delta)^2}{4\mu c\delta}. \quad (31)$$

Motivated by the operational calculus approach described in [7], we can write the general solution $p_{m,n}$ as the sum of two contour integrals in the form

$$p_{m,n} = \int_{C_1} P_1(\mu) \lambda_1^m \mu^n d\mu + \int_{C_2} P_2(\mu) \lambda_2^m \mu^n d\mu, \quad (32)$$

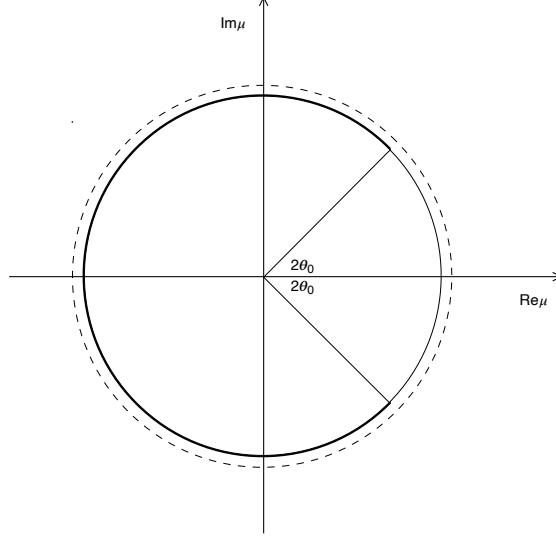


Figure 3: The branch cut, denoted by the heavy curve, and the contour C_1 , denoted by the dotted curve, in the complex μ plane.

where $\lambda_1(\mu), \lambda_2(\mu)$ are the roots of (30) and P_1, P_2 and the contours C_1, C_2 need to be chosen to satisfy conditions (27, 28). Taking

$$\lambda_1 = S - \sqrt{S^2 - 1}, \quad \lambda_2 = S + \sqrt{S^2 - 1}, \quad (33)$$

where the square roots will be defined below, we see that both λ_1 and λ_2 are analytic functions of μ except for possible branch points at $S(\mu) = \pm 1$. The value $S = 1$ corresponds to the double root $\mu = 1$ and $S = -1$ corresponds to the pair of complex conjugate roots at the branch points of $\lambda_1(\mu), \lambda_2(\mu)$. At these branch points, $\mu = e^{i\theta}$ where, from (31), (33), $\theta = 2\theta_0$ with $\cos \theta_0 = \frac{c - \delta}{c + \delta}$. The complex μ -plane is therefore cut along the circle $|\mu| = 1$ for $2\theta_0 < \theta < 2\pi - 2\theta_0$, as shown in Figure 3, and we define the square roots to be such that

$$\lambda_1 \sim \frac{4c\delta}{(c + \delta)^2\mu}, \quad \lambda_2 \sim \frac{(c + \delta)^2\mu}{4c\delta} \quad (34)$$

as $|\mu| \rightarrow \infty$.

75 Since the only singularities of $\lambda_1(\mu), \lambda_2(\mu)$ are on the unit circle, it is appropriate to choose C_1 and C_2 as closed contours on which $|\mu| > 1$. As $|\mu| \rightarrow \infty$, the integrand

in the second integral of (32) is proportional to μ^{m+n} ; hence this integral represents an unacceptable wave travelling from infinity in the negative X -direction and so $P_2 \equiv 0$. The first integral depends on μ^{n-m} as $|\mu| \rightarrow \infty$ and will be zero if $m > n$ assuming
80 that P_1 decays at infinity. Thus this integral is zero ahead of the leading characteristic whose mean speed is c_{AV} .

If we take C_1 to be a circle of radius slightly greater than 1 as shown in Figure 3, we see that, in order to satisfy (28) and noting that $\lambda_1(1) = 1$, we must choose

$$P_1 = \frac{1}{2\pi i(\mu - 1)}. \quad (35)$$

To carry out the asymptotic evaluation of (32) for large m, n and hence to compare with the theory of Section 2, we write

$$\lambda_1^m \mu^n = \exp(m \log \lambda_1 + n \log \mu) \quad (36)$$

to see that the major contribution to the integral as $m, n \rightarrow \infty$ will come from the saddle points where

$$\frac{m}{n} = -\frac{\lambda_1(\mu)}{\mu \lambda_1'(\mu)}. \quad (37)$$

Following the approach of [10], we see that the solution will comprise modulated wave packets each moving to the right with a group velocity determined by (37).

The largest modulation will occur when m, n satisfy (37) at the pole where $\mu = 1$. This happens when

$$\frac{m}{n} = \frac{2\sqrt{c\delta}}{c + \delta}, \quad (38)$$

which corresponds to $X = c_H T$, where c_H is defined by (22) and in this case is
85 $\frac{(1+c)\sqrt{c\delta}}{c+\delta}$. A similar analysis to that used in [7] shows that the local solution near such values of m, n is described by the integral of an Airy function of the first kind and this behaviour will be displayed explicitly in the computations in Section 4.

We also remark that the integral representation of $u_{m,n}$ that corresponds to (32) can be found by returning to (25), (29) and noting that

$$\frac{U}{P} = \frac{(c + \delta)\mu - 2\delta\lambda - c + \delta}{(c + \delta)\mu - 2c\lambda + c - \delta}. \quad (39)$$

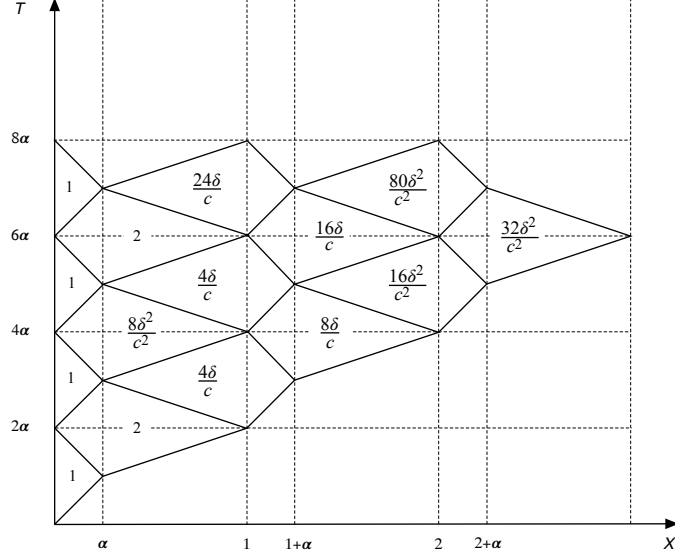


Figure 4: The lowest order term for pressure as $\delta \rightarrow 0$ given by (25, 26) for small values of m, n when $\alpha = \frac{1}{1+c}$.

Using (30, 31) it can be shown that the denominator in this expression has a simple zero at $\mu = -1$ and a double zero at $\mu = 1$. Moreover as $\mu \rightarrow 1$,

$$\frac{U}{P} \rightarrow \sqrt{\delta/c}. \quad (40)$$

Thus $u_{m,n}$ is proportional to $p_{m,n}$ as $m, n \rightarrow \infty$, but it is an order of magnitude smaller.

3.2. The Limit as $\delta \rightarrow 0$

90 We now return to the asymptotic limit when δ is small and $c_H = O(\sqrt{\delta})$, so that the initial wave motion described by (25), (26) is as shown in Figure 4. This figure indicates that the disturbance rapidly becomes localised near $X = 0$ as $\delta \rightarrow 0$. A similar figure would describe the early response when the boundary pressure is applied to a water layer at $X = \alpha$, the only significant difference being that the maximum pressure would
 95 always be less than 2.

To analyse the solution (32) when δ is small, we write $\mu = e^{i\theta}$ so that

$$S = \frac{\cos \theta - \cos^2 \theta_0}{\sin^2 \theta_0}. \quad (41)$$

Hence $|S| < 1$ when $0 < \theta < 2\theta_0$ and $2\pi - 2\theta_0 < \theta < 2\pi$. This implies that $\lambda_1(\mu)$ has unit modulus for these ranges of θ and is real and less than -1 otherwise.

When $\delta \ll 1$, we find that S is $O(1)$ when θ and $(2\pi - \theta)$ are $O(\sqrt{\delta})$ but, away from these regions, S is $O(c/\delta)$ and so λ_1 is $O(\delta/c)$. Thus, as anticipated before (38), when the integral in (32) is taken around a contour just outside the unit circle and n is large, the main contribution is from the region where $|\mu - 1|$ is $O(\sqrt{\delta})$. Writing $\mu = 1 + i\sqrt{\delta}\tilde{\theta}$, we find that $p_{m,n}$ can be written asymptotically in terms of a principal value integral as

$$p_{m,n} \sim \frac{1}{2\pi i} \oint_{-\infty}^{\infty} \lambda_1^m \exp(i(n+1)\sqrt{\delta}\tilde{\theta}) \frac{d\tilde{\theta}}{\tilde{\theta}} + \frac{1}{2}, \quad (42)$$

where the last term is the contribution to the integral from a small semicircle around the pole at $\mu = 1$. When $m = 0$, the principal value integral is $\frac{1}{2}$, so that $p_{m,n}$ satisfies
 100 (28). However the behaviour for $m > 0$ is more difficult to discern since λ_1 is real or complex depending on the sign of $\tilde{\theta}^2 - 4\theta_0^2$.

This analysis reveals a significant difference between the homogenisation of the small- δ problem and the homogenisation when $\delta = O(1)$. In the latter case, the argument used in [7] reveals that homogenisation is only possible when $n \gg O(1)$, with
 105 different homogenisations occurring close to and away from the wavefront moving with speed c_H . Now, however, we see from (42) that when n is $O(1/\sqrt{\delta})$, we effectively retrieve a lowest-order solution of the same form as that when n, m are of $O(1)$; it is only when $n \gg O(1/\sqrt{\delta})$ and $m \gg 1$ that the oscillatory variation from one cell to the next is small enough for homogenisation to apply. This observation is consistent with
 110 the result in the Appendix that A is of $O(\sqrt{\delta})$. Hence the Airy function solution in this case will apply when $\hat{t} = O(1/\sqrt{\delta})$, implying that T must greatly exceed $1/\sqrt{\delta}$, and these predictions will be confirmed by the numerical results shown in Figure 10 in Section 4.

3.3. Small and large air/water fractions

As shown in Figure 1, c_H depends most sensitively on α when either α or $(1 - \alpha)$ is
 115 of $O(\delta)$, and the region of the (X, T) plane in which our homogenisation is valid will change accordingly. For example, when α is of $O(\delta)$ so that water occupies most of the region of interest, then $c_H^2 \simeq \frac{\delta c^2}{\delta + \alpha c^2} \sim O(1)$. However, as shown in the Appendix,

the constant A in (23) is then of $O(1)$ so that we expect there to be no change in the
 120 scalings needed to achieve large-time homogenisation. We henceforth concentrate on
 the regime where α and δ are both small and comparable and X and T are at most of
 $O(\delta^{-1})$ before briefly mentioning the case when $(1 - \alpha)$ is small.

When δ is zero, the water boundary at $X = \alpha$ acts as a perfect reflector, and the
 waves in the first air layer, $0 < X < \alpha$, comprise oscillations travelling at unit speed
 and there is no large-time homogenisation. However, when $0 < \delta \ll 1$, some of the
 energy leaks out into the water. Before any reflections from the next interface occur we
 find that the outgoing wave solution is constant in thin strips and is given by

$$p = 1 - (-1)^n \left(\frac{1 - \delta/c}{1 + \delta/c} \right)^n \quad (43)$$

when $\alpha \leq X \leq 1$ and $-(2n+1)c\alpha < X - cT - \alpha < -(2n-1)c\alpha$. Thus, after a transient
 when T is $O(1)$, when $n \rightarrow \infty$ we observe modulated harmonic oscillations in the water
 of the form

$$p \sim 1 \pm \exp\left(-\frac{\delta(cT - X)}{\alpha c^2}\right) \quad (44)$$

and this holds for $cT \leq X \leq 2 - cT$. and is displayed in Figure 5 for the case $c = 3$.
 The derivation of this Figure (and also Figure 6) will be described in Section 4.

Next we consider what happens in the narrow air layer $1 < X < 1 + \alpha$. Again we
 can calculate the reflected and the transmitted wave generated by the incident wave (43)
 at the interfaces at $X = 1$ and $X = 1 + \alpha$ to find

$$p_{ref} = (-1)^m \left(\frac{1 - \delta/c}{1 + \delta/c} \right)^m - \left(\frac{1 - \delta/c}{1 + \delta/c} \right)^{2m} \quad (45)$$

for $\alpha < X < 1$ and $2 + (2m-1)c\alpha < X + cT + \alpha < 2 + (2m+1)c\alpha$. and

$$p_{trans} = 1 - \left(\frac{1 - \delta/c}{1 + \delta/c} \right)^{2n+1} - (-1)^n \frac{2\delta/c}{(1 + \delta/c)} \left(\frac{1 - \delta/c}{1 + \delta/c} \right)^n \quad (46)$$

125 for $X > 1 + \alpha$ and $2\alpha - 2(n+1)c\alpha < X - cT, 2\alpha - 2nc\alpha$. As expected, as $\delta \rightarrow 0$,
 $p_{trans} \rightarrow 0$ and it can be shown that as $m, n \rightarrow \infty$, the amplitude of the oscillations of p
 are exponential functions of $X \pm cT$ in agreement with Figure 6.

Numerical results in the next section reveal that, for even longer times, all the high
 frequency waves of amplitude $O(1)$ are trapped in the region $0 < X < 1$; this happens

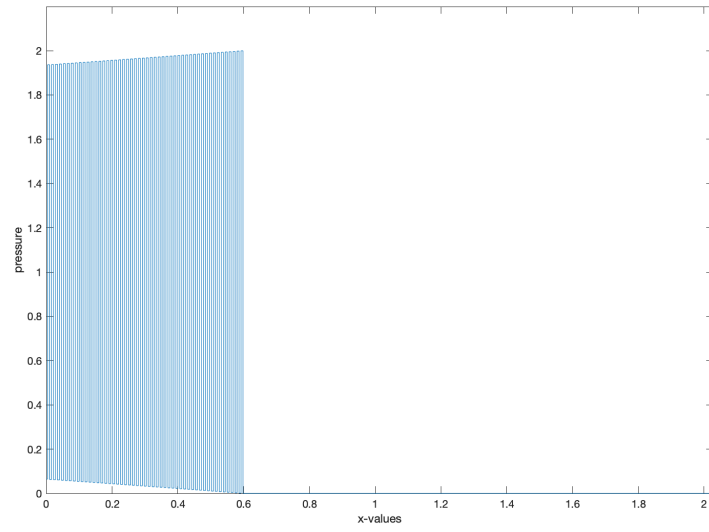


Figure 5: Pressures at $T = 0.2$ with $\alpha = 10^{-3}$.

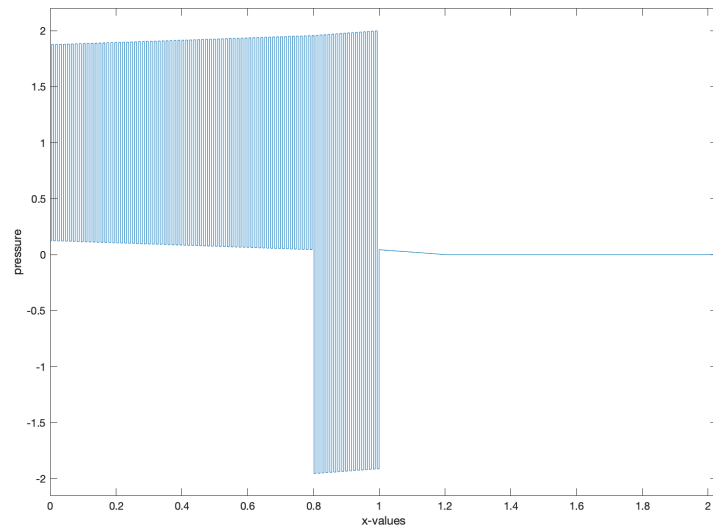


Figure 6: Pressures at $T = 0.4$ with $\alpha = 10^{-3}$.

130 because the small density ratio makes the interface $X = \alpha$ a nearly-perfect transmitter and the interface $X = 1$ a nearly-perfect reflector. The outgoing high-frequency waves have mean approximately 1 and the reflected waves have mean approximately -1 while the non-oscillatory wave penetrating the water in $X > 1 + \alpha$ has amplitude of $O(\delta)$ when T is $O(1)$.

135 When there are several air layers, as in Figures 11 and 12 in Section 4, numerical calculations reveal a more and more complicated pattern of oscillations in $0 < X < 1$ and a smoothly varying pressure in $X > 1$ whose mean approaches 1 as $T \rightarrow \infty$ with $X \leq c_H T$.

Although these calculations become more difficult as X and T increase, it is still possible to work out the variation in pressure from one side of the narrow air layer to the other. Working on the scale where X, T are $O(1)$ or greater, the air gaps can, to lowest order in δ , be regarded as line discontinuities at $X = n$ in the equations for the water. Across these discontinuities, (1, 2, 4, 5) show that, assuming a smooth homogenisation,

$$\left[\frac{\partial p_w}{\partial X} \right]_n = -\frac{1}{\delta} \left[\frac{\partial u_w}{\partial T} \right]_n = -\frac{1}{\delta} \left[\frac{\partial u_a}{\partial T} \right]_n = \frac{1}{\delta} \left[\frac{\partial p_a}{\partial X} \right]_n \simeq \frac{\alpha}{\delta} \frac{\partial^2 p_a}{\partial X^2} = \frac{\alpha}{\delta} \frac{\partial^2 p_a}{\partial T^2} = \frac{\alpha}{\delta} \frac{\partial^2 p_w}{\partial T^2} \quad (47)$$

to lowest order, where $[]_n$ indicates the change from $X = n$ to $X = n + \alpha$. Also, under this assumption,

$$[p_w]_n \simeq \delta \alpha \frac{\partial p_w}{\partial X}. \quad (48)$$

Thus, to lowest order in δ , the pressure is continuous across an air layer and has a discontinuity in slope of $O(1)$. From (22), we see that c_H will be $O(\sqrt{\delta})$ unless $\alpha = O(\delta)$, in which case

$$c_H^2 \simeq \frac{c^2 \delta}{\delta + c^2 \alpha}, \quad (49)$$

which is of $O(1)$. We can then discern the homogenisation by using (47) when $\alpha \sim \delta \ll 1$. The fact that $\frac{\partial p}{\partial X}$ has a jump of size $\frac{\alpha}{\delta} \frac{\partial^2 p}{\partial T^2}$ across each narrow air layer means that in the water

$$\frac{\partial^2 p}{\partial X^2} - \frac{1}{c^2} \frac{\partial^2 p}{\partial T^2} = \sum_{n=1}^{\infty} \frac{\alpha}{\delta} \frac{\partial^2 p}{\partial T^2} D(X - n), \quad (50)$$

where $D(X)$ is the Dirac delta function. Thus, on an even longer time and space scale,

the equation may be homogenised to become

$$\frac{\partial^2 p}{\partial x^2} - \frac{1}{c^2} \frac{\partial^2 p}{\partial t^2} - \frac{\alpha}{\delta} \frac{\partial^2 p}{\partial t^2} = 0, \quad (51)$$

which is exactly equivalent to (18) with c_H given by (49).

140 An extension of the calculation in the Appendix to the case where α is small and of $O(\delta)$ will not be detailed here, but it reveals that the coefficient A in (23) is of $O(1)$. Hence the dispersed wave profile near $x = c_H t$ has a similar profile to that when α is of $O(1)$ and this is illustrated in Figure 12. However, when α tends to zero with $\delta > 0$, A also tends to zero and the wave is not dispersive.

145 The above approach can also be applied when $1 - \alpha$ is small rather than α . The major difference is that the boundary $X = \alpha$ of the first water layer has a very small reflection coefficient and so high-frequency oscillations are not trapped in $X < 1$.

3.4. A Continuous Solution

We conclude this section by noting that the solution (32) subject to (27, 28) is special in that the exact solution is piecewise constant in each (m, n) cell. In contrast, for a continuous boundary condition, the solution will have jump discontinuities in the first derivatives of p and u at each air/water interface. We can illustrate such a case by noting that

$$\hat{p} = \int_0^T p dT, \quad \hat{u} = \int_0^T u dT \quad (52)$$

satisfy equations (1, 2, 4, 5) with $\hat{p} = T$ on $X = 0$ and $\hat{p} = \hat{u} = 0$ at $T = 0$. This implies that, in either air or water, using (13, 14),

$$\frac{\partial \hat{p}}{\partial X} = \int_0^T \frac{\partial p}{\partial X} dT = -\rho u \quad (53)$$

and

$$\frac{\partial \hat{u}}{\partial X} = \int_0^T \frac{\partial u}{\partial X} dT = -\frac{1}{K} p, \quad (54)$$

which shows how the jump discontinuities depend on δ and c . We also note that the
150 dispersed waveform near $X = c_H T$ involves a double integral of an Airy function.

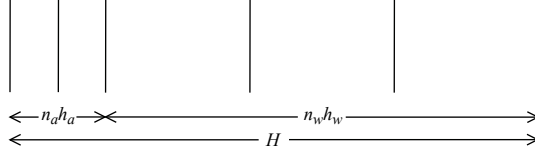


Figure 7: A single period with 5 cells in a periodic Goupillaud medium with $n_a = 2$ and $n_w = 3$.

4. Numerical Simulations

This section describes simulations for several piecewise-constant Goupillaud media including one example of a random medium. In our Goupillaud media, material properties are constant within spatial cells whose lengths are such that waves have equal
155 transit times across each cell. All the simulations are exact to within floating point rounding errors. Goupillaud media have been used previously to obtain exact solutions for comparison with analytical results, for example in [5].

4.1. Periodic Goupillaud media

We construct a periodic Goupillaud medium as follows. We suppose there are n_a air
160 cells followed by n_w water cells in each period of length H . Also, in this section only, we denote the sound speeds in air and water by c_a and c_w . Given these parameters, we denote the length of each air and water cell by h_a and h_w , which satisfy the Goupillaud constraints $c_a \Delta = h_a$, $c_w \Delta = h_w$, where Δ is the time step. Also $n_a h_a + n_w h_w = H$ and the air fraction $\alpha = n_a c_a / (n_a c_a + n_w c_w)$. In the previous sections we specified α as the
165 principal geometric parameter but we now use α to find n_a and n_w under the inherent Goupillaud assumption that $c_a(1 - \alpha)/c_w \alpha$ is a rational number. Figure 7 shows an illustration of a single period in a periodic Goupillaud medium.

When the medium has the Goupillaud property, we can compute the exact solution of the wave equations (13) and (14) using the Godunov method with a unit Courant
170 number. This method, described in [11], uses a sequence of local Riemann problems to iterate a piecewise constant solution on the Goupillaud grid of cells which is exact when the Courant number ($c_a \Delta / h_a$ or $c_w \Delta / h_w$) is unity in each cell.

4.2. Simulations for periodic Goupillaud media with $p(0, t) = 1$ for $t > 0$

For the purposes of comparison with the previous sections, and for simplicity, we
 175 will henceforth set $c_a = 1$ and $c_w = 3$, which is equivalent to taking $c = 3$. We also
 take $\delta = \rho_{a0}/\rho_{w0} = 10^{-3}$.

4.2.1. Example 1, $\alpha = 0.25$

Consider the case with $H = 1$ and two cells in each period, such that $n_a = n_w = 1$,
 $h_a = 0.25$, $h_w = 0.75$, which corresponds to the problem described in Section 3. The
 180 medium is Goupillaud with a cell time step, $\Delta = 0.25$, a duration of 0.5 to traverse each
 period and $\alpha = 0.25$. For the simulations, the length of the medium, L , is the total
 number of spatial periods. The boundary conditions are $p(0, t) = 1$ and $p(L, t) = 0$, and
 L is set large enough for reflections from the boundary at $x = L$ not to occur over the
 times covered. The first cell in each period is an air cell.

185 At times that are even multiples of Δ , the Godunov solution in neighbouring air and
 water cells in two adjacent periods is equal to $p_{m,n}$, the solution given in Section 3.1.
 The time step in the difference equations of Section 3.1 is twice that of the Godunov
 time step. In the figures, integer values of X correspond to the boundaries between
 the spatial periods and the cross on the axis denotes the point $c_H T$ where, from (22),
 190 $c_H = 0.0730$. Note that the times stated in the figures are integer multiples of Δ , which
 are equivalent to the values of T .

Figures 8 to 10 show the pressures at $T = 25$, 250 and 1000, revealing quite strik-
 ingly the retardation of the front caused by the small density ratio of $\delta = 10^{-3}$. Although
 the solution is near to its homogenised waveform for $T > 250$, these figures reveal the
 195 gradual appearance of the maximum just trailing the front as predicted by the earlier
 asymptotic analysis.

4.2.2. Example 2, $\alpha = 10^{-3}$

We next consider the example from Section 3.3 where α and δ are both 10^{-3} . The
 medium is Goupillaud again, with $H = 1$, but now with 334 cells in each period, such
 200 that $n_a = 1$ and $n_w = 333$; this gives $h_a = 10^{-3}$, $h_w = 3 \times 10^{-3}$ and $\Delta = 10^{-3}$.

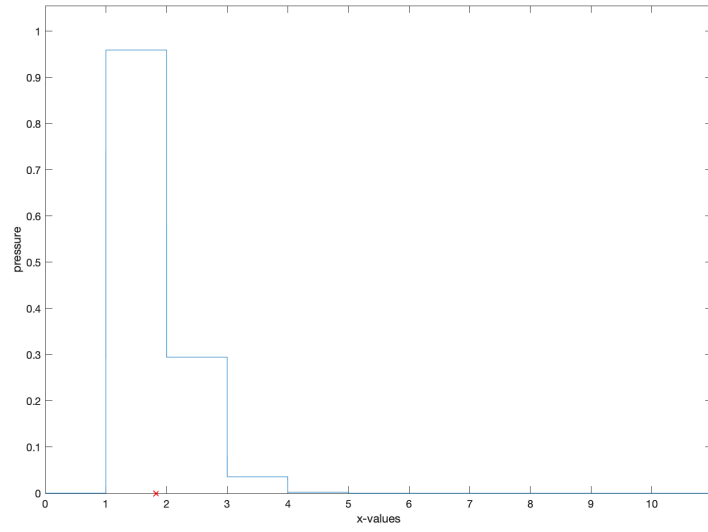


Figure 8: Pressures at $T = 25$ for $\alpha = 0.25$ with $n_a = n_w = 1$ and $\delta = 10^{-3}$.

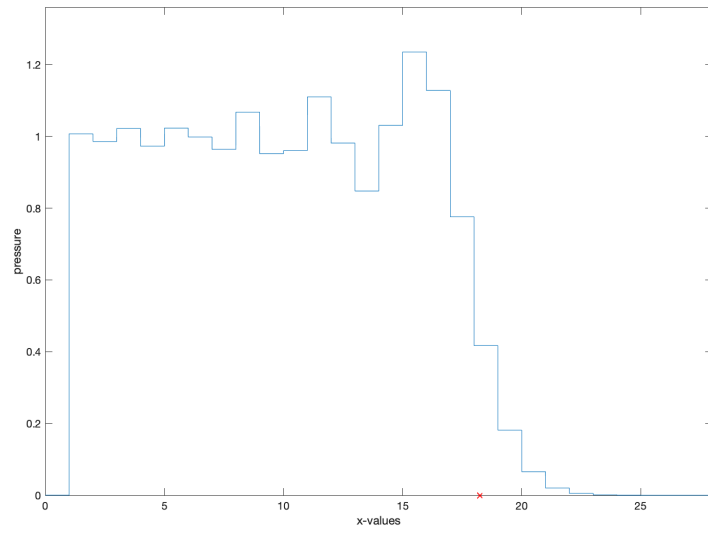


Figure 9: Pressures at $T = 250$ for $\alpha = 0.25$ with $n_a = n_w = 1$ and $\delta = 10^{-3}$.

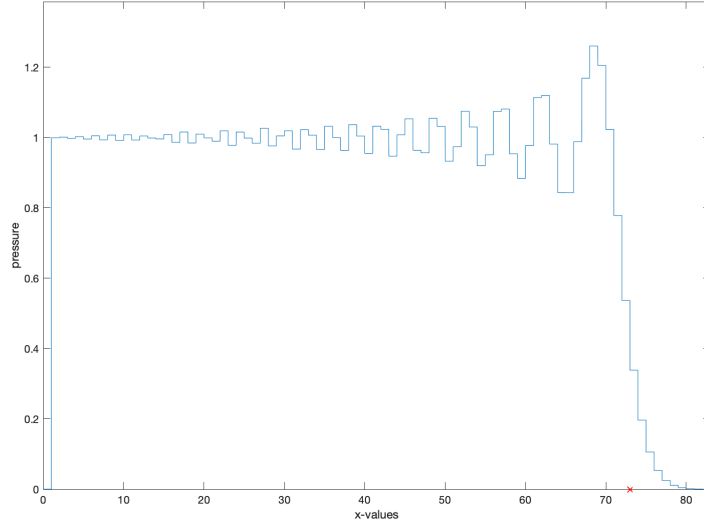


Figure 10: Pressures at $T = 1000$ for $\alpha = 0.25$ with $n_a = n_w = 1$ and $\delta = 10^{-3}$.

In Section 3.3 we showed that when $\alpha, \delta \ll 1$, the solution may be homogenised when $T \gg O(\delta^{-\frac{1}{2}})$ as is borne out by these simulations. In Figure 11 we show the pressure at a time of $T = 8$, which requires 8000 Godunov time steps. Figure 12 shows the pressure at a time of $T = 32$ requiring 32,000 Godunov time steps. These results show the existence of a region near the origin in which there are persistent high-frequency oscillations, which reflects the modification of the homogenisation shown in Section 3.3. The homogenised wave speed is now $c_H = 0.9492$ and the point $c_H T$ is again indicated on Figures 11 and 12.

4.3. Random Goupillaud media

One way of defining a random Goupillaud medium is to specify (i) N , the total number of cells (ii) c_i , the sound speed in the i -th cell for $i = 1 \dots N$ and (iii) Δ , the time step. The cell widths h_i are in accordance with the Goupillaud constraints $c_i \Delta = h_i$ for each i and the domain length is defined by $L = \sum_{i=1}^K h_i$. We then assume that the cells are chosen independently to be air with probability π_a and water with probability

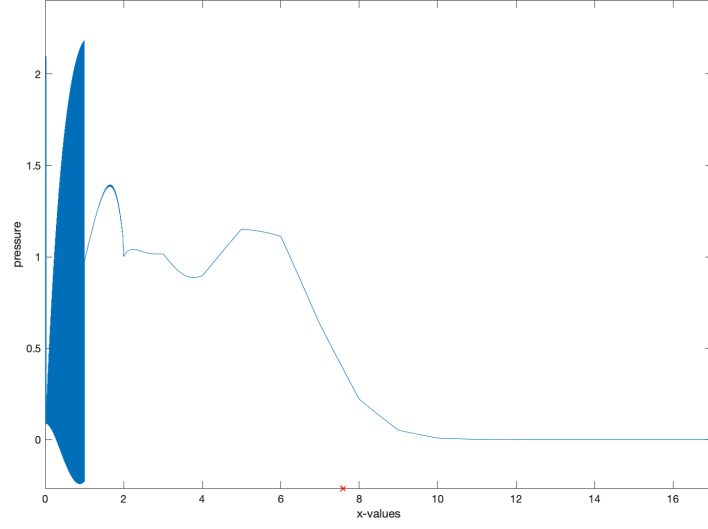


Figure 11: Pressures at $T = 8$ for $\alpha = 10^{-3}$ with $n_a = 1$, $n_w = 333$ and $\delta = 10^{-3}$.

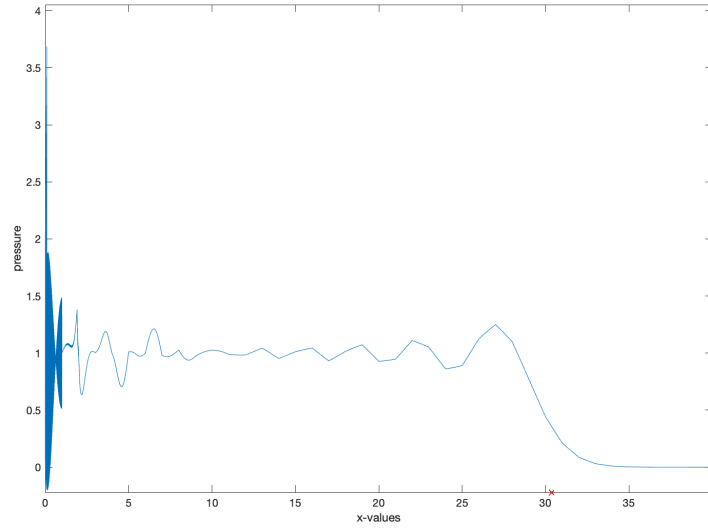


Figure 12: Pressures at $T = 32$ for $\alpha = 10^{-3}$ with $n_a = 1$, $n_w = 333$ and $\delta = 10^{-3}$.

215 π_w . To specify these probabilities it is convenient to assume that the positive integers n_a and n_w are specified such that $\pi_a = n_a/(n_a + n_w)$ and $\pi_w = n_w/(n_a + n_w)$ so that $\pi_a + \pi_w = 1$. The numbers of air and water cells, N_a and N_w are then binomial random variables with means $N\pi_a$ and $N\pi_w$. Once a realisation of the domain properties has been sampled, N_a can be counted and $N_w = N - N_a$.

Wood's law can still be derived from (19) to give $c_H = \sqrt{K_R/\rho_R}$, where the average density ρ_R and modulus K_R are given by $\rho_R(N_a h_a + N_w h_w) = N_a h_a \rho + N_w h_w$ and

$$\frac{N_a h_a + N_w h_w}{K_R} = \frac{N_a h_a}{K_a} + \frac{N_w h_w}{K_w};$$

220 here $K_a = 1$ and $K_w = 9 \times 10^3$ as defined in (9, 10), and the total fraction of air is given by $\alpha = N_a c_a / (N_a c_a + N_w c_w)$. Note that c_H , ρ_R , K_R and α are now random variables.

We now specialise to the case where $n_a = n_w = 1$, $h_a = 0.25$, $h_w = 0.75$, $c_a = 1$, $c_w = 3$, with $\rho = 10^{-3}$. The time step is $\Delta = 0.25$ and the first cell is an air cell. This example is then a randomised version of the first periodic example where the total
225 number of cells is specified, but not the length of the whole domain. The sample values vary from realisation to realisation but the variance is small as a result of the thousands of cells involved.

Figure 13 shows the pressure for wave propagation in a random Goupillaud medium as specified above at time $T = 2500$. The sample value of the average sound speed
230 using Wood's law is $c_H = 0.07313$. We see that although the characteristic "front" of the disturbance still travels with speed c_H , the previously-observed dispersion near this front is no longer present. This is an example of how wave propagation in periodic composite media can be altered substantially when random perturbations are made to the periodicity. For a review of known results concerning wave propagation in random
235 media see [12].

5. Conclusion

We have shown that homogenisation theory confirms the validity of Wood's Law for the sound speed of pressure waves in an air/water mixture, and explains how the small density ratio causes this sound speed to be much less than the speed in either

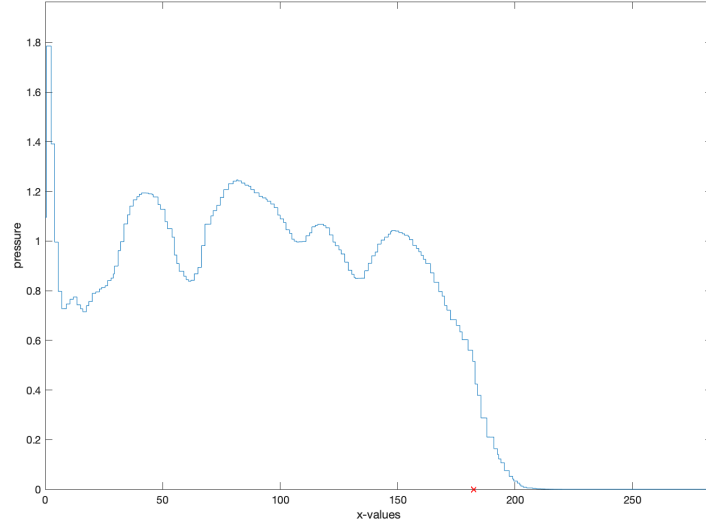


Figure 13: Pressures at $T = 2500$ in a random Goupillaud medium where the cross marks the point $c_H T$.

240 air or water. We have also shown that this modifies the new regions in space-time over which homogenisation is applicable. Also we find that, when the air fraction is small, persistent ringing can occur with a slowly-varying exponential time-dependent amplitude.

Throughout, we have chosen parameter values that are such that the composite is a
 245 Goupillaud medium which means that the equations can be discretised to give solutions that are exact to within rounding errors. This has enabled us to compare the theory with exact numerical solutions as well as to contrast the response of a random Goupillaud medium with that of a deterministic periodic medium.

Appendix

In order to derive equation (23), we follow the analysis in [7] and start by writing $p = p(X, \zeta, \hat{t}), u = u(X, \zeta, \hat{t})$ where $\zeta = x - c_H t$ and $t = \tau^2 \hat{t}$. Then (13) and (14)

become

$$K \frac{\partial u}{\partial X} + \frac{K}{\tau} \frac{\partial u}{\partial \zeta} - \frac{c_H}{\tau} \frac{\partial p}{\partial \zeta} + \frac{1}{\tau^3} \frac{\partial p}{\partial \hat{t}} = 0$$

and

$$\frac{\partial p}{\partial X} + \frac{1}{\tau} \frac{\partial p}{\partial \zeta} - \frac{c_H \rho}{\tau} \frac{\partial u}{\partial \zeta} + \frac{\rho}{\tau^3} \frac{\partial u}{\partial \hat{t}} = 0,$$

and, when we expand p, u as in (12), we find that p_0, u_0 are functions of ζ, \hat{t} alone. The next-order equations are

$$\frac{\partial u_1}{\partial X} + \frac{\partial u_0}{\partial \zeta} - \frac{c_H}{K} \frac{\partial p_0}{\partial \zeta} = 0$$

and

$$\frac{\partial p_1}{\partial X} + \frac{\partial p_0}{\partial \zeta} - c_H \rho \frac{\partial u_0}{\partial \zeta} = 0.$$

Thus

$$\frac{\partial u_0}{\partial \zeta} = \frac{c_H}{K_H} \frac{\partial p_0}{\partial \zeta}$$

and, remembering that (19) still holds,

$$p_1 = (J_1(X) - \overline{J_1}) \frac{\partial p_0}{\partial \zeta},$$

where $J_1(X) = \int_0^X \left(\frac{\rho}{\rho_{AV}} - 1 \right) dX$, and

$$u_1 = \frac{c_H}{K_H} \left(J_2(X) - \overline{J_2} \right) \frac{\partial p_0}{\partial \zeta},$$

250 where $J_2 = \int_0^X \left(\frac{K_H}{K} - 1 \right) dX$ and $J_1 = -\beta J_2$ with $\beta = \frac{(1-\delta)(\alpha c^2 + (1-\alpha)\delta)}{(c^2 - \delta)(\alpha\delta + 1 - \alpha)}$.

Repeating this process, we can determine p_2 and u_2 similarly as

$$p_2 = (J_3(X) - \overline{J_3}) \frac{\partial^2 p_0}{\partial \zeta^2}$$

and

$$u_2 = \frac{c_H}{K_H} (J_4(X) - \overline{J_4}) \frac{\partial^2 p_0}{\partial \zeta^2},$$

where $J_3 = -\int_0^X \left(\beta + \frac{\rho}{\rho_{AV}} \right) (J_2 - \overline{J_2}) dX$, and $J_4 = -\int_0^X \left(1 + \frac{K_H \beta}{K} \right) (J_2 - \overline{J_2}) dX$.

Finally, in order to avoid secular terms in $\frac{\partial u_3}{\partial \zeta}$ and $\frac{\partial p_3}{\partial \zeta}$, we end up with the equation

$$A \frac{\partial^4 p_0}{\partial \zeta^4} = \frac{\partial^2 p_0}{\partial \hat{t} \partial \zeta}$$

where

$$A = c_H K_H \left(\frac{1}{K} (J_3 - \overline{J_3}) \right).$$

The parameter A is of $O(1)$ when $\delta = O(1)$. However, as $\delta \rightarrow 0$, when $c_H^2 \sim \frac{\delta}{\alpha(1-\alpha)}$, we find that, to lowest order,

$$J_3(X) = \begin{cases} -\frac{1}{2}X(X-\alpha) & \text{for } 0 < X < \alpha \\ \frac{1+\alpha}{2(1-\alpha)}(1-X)(X-\alpha) & \text{for } \alpha < X < 1 \end{cases}$$

and

$$\overline{J_3} = \frac{1}{12} (1 - \alpha - \alpha^2).$$

Hence A is of $O(\sqrt{\delta})$ when α is not close to 0 or 1. As can be seen from (22), this calculation is not uniformly valid when $\alpha \rightarrow 0$; the integral J_3 needs to be recalculated and it can be shown that A is of $O(1)$ when α is of $O(\delta)$.

Acknowledgement

This research did not receive any specific grant from funding agencies in the public, commercial, or not-for-profit sectors.

References

- [1] J.R. MACDONALD, *Some simple isothermal equations of state*. Rev. Mod. Phys., 38 (4) (1966) 669-679.
- [2] A.B. WOOD, *A Textbook of Sound, 1st ed.* Macmillan, New York, 1930.
- [3] A. MALLOCK, *The damping of sound by frothy liquids*. Proc. Royal Soc. A. 84 (572) (1910) 391-395.
- [4] P.S. WILSON AND R.A. ROY, *An audible demonstration of the speed of sound in bubbly liquids*. Am. J. Phys. 76 (10) (2008) 975-981.
- [5] F. SANTOSA, AND W.W. SYMES, *A dispersive effective medium for wave propagation in periodic composites*. SIAM J. Appl. Math. 51 (4) (1991) 984-1005.

- 270 [6] M. QUEZADA DE LUNA, AND D.I. KETCHESON *Two-dimensional wave propaga-*
tion in layered periodic media. SIAM J. Appl. Math. 74 (6) (2014) 1852-1869.
- [7] H. OCKENDON, J.R. OCKENDON, C.L. FARMER, AND D.J. ALLWRIGHT, *One-*
dimensional wave dispersion in layered media. SIAM J. Appl. Math. 75 (5) (2015)
2128-2146.
- [8] C.L. FARMER, H. OCKENDON, J.R. OCKENDON *Wave propagation along peri-*
275 *odic Layers.* SIAM J. Appl. Math. 78 (4) (2018) 2154-2175.
- [9] C.E. BRENNEN, *Cavitation and Bubble Dynamics.* Oxford University Press, New
York, 1995.
- [10] F.W.J. OLVER, *The asymptotic solution of linear differential equations of the sec-*
ond order for large values of a parameter. Phil. Trans. R. Soc.A. 247 (1954) 307-
280 327.
- [11] R.J. LEVEQUE, *Finite Volume Methods for Hyperbolic Problems.* Cambridge Uni-
versity Press, 2002.
- [12] J.-P. FOUQUE, J. GARNIER, G. PAPANICOLAOU, AND K. SØLNA, *Wave Propaga-*
tion and Time Reversal in Randomly Layered Media. Springer-Verlag New York,
285 2007.